Multisensory integration enhances audiovisual responses in the Mauthner cell

Santiago Otero-Coronel[1], Thomas Preuss[2] and Violeta Medan[1,3]*

Abbreviated title: Multisensory integration in the Mauthner cell

1. Instituto de Fisiología y Biología Molecular y Celular, Consejo Nacional de Investigaciones Científicas y Tecnológicas, Buenos Aires, Argentina (1428).
2. Dept. Psychology, Hunter College, City University of New York, New York, NY, USA (10065).
3. Dept. Fisiología y Biología Molecular y Celular, Facultad de Ciencias Exactas y Naturales, Universidad de Buenos Aires, Buenos Aires, Argentina (1428).

*Corresponding author, e-mail: violetamedan@fbmc.fcen.uba.ar.

ACKNOWLEDGEMENTS

This work was supported by PICT 2012-1578 and PICT 2017-0007, FONCYT-ANPCYT (VM), PIP 11220130100729CO (VM), UBACyT 20020130300008BA (VM), Thalmann Program, University of Buenos Aires (VM) SOC was supported by undergraduate fellowships from the National Interuniversity Council and University of Buenos Aires. The authors thank Dr. Lidia Szczupak and members of the Medan lab for discussion and for reading previous versions of this manuscript. The current address of SOC is at The Rockefeller University, New York, NY, USA (10065).

ABSTRACT

Multisensory integration combines information from multiple sensory modalities to create a coherent perception of the world. In contexts where sensory information is limited or equivocal, it also allows animals to integrate individually ambiguous stimuli into a clearer or more accurate percept and, thus, react with a more adaptive behavioral response. Although responses to multisensory stimuli have been described at the neuronal and behavioral levels, a causal or direct link between these two is still missing. In this study, we studied the integration of audiovisual inputs in the Mauthner cell, a command neuron necessary and sufficient to trigger a stereotypical escape response in fish. We performed intracellular recordings in adult goldfish while presenting a diverse range of stimuli to determine which stimulus properties affect their integration. Our results show that stimulus modality, intensity, temporal structure, and interstimulus delay affect input summation. Mechanistically, we found that the distinct decay dynamics of feedforward inhibition triggered by auditory and visual stimuli can account for certain aspects of input integration. Altogether, this is a rare example of the characterization of multisensory integration in a cell with clear behavioral relevance, providing both phenomenological and mechanistic insights into how multisensory integration depends on stimulus properties.

SIGNIFICANCE STATEMENT

Animals integrate multiple sources of information in order to form a percept of the world that allows adaptive behavioral decisions. The current study demonstrates the cellular mechanism that underlies hall-mark features of multimodal integration in individual reticulospinal neurons. Since the Mauthner cells initiate the startle escape response, this characterization emphasizes the role of single neurons in multimodal decision-making. Elucidating the principles and mechanisms by which different senses interact might prove useful in designing or optimizing the sensory environment of people performing perceptually demanding tasks, including individuals with sensory disabilities.

53 INTRODUCTION

54 The ability to detect a potential threat and react with an escape behavior is critical for survival. In
55 nature, however, many predators develop strategies such as camouflage or partial hiding to decrease
56 their salience, and sensory stimuli tend to be noisy and ambiguous. Consequently, it is adaptive for
57 animals to have ways to disambiguate the signals from the sensory inflow they receive, especially in
58 contexts where available information is limited.

59 One strategy for reducing sensory uncertainty is multisensory integration (MSI), which is defined as
60 the process of combining information coming from multiple sensory streams to form a new percept
61 with reduced ambiguity (Stein and Stanford, 2008). MSI has been extensively documented in animals
62 from nematodes to humans and in a broad range of behavioral contexts (Wallace et al., 1998;
63 Metaxakis et al., 2018; Zhou et al., 2019; Gil-Guevara et al., 2022). In the context of escape behaviors,
64 MSI of threat-like stimuli increases the escape probability and reduces the latency of the evoked
65 response (Rowland et al., 2007; Martorell and Medan, 2022). In mammals, activation of different parts
66 of the superior colliculus determines whether animals engage in exploratory or defensive behaviors
67 (Dean et al., 1989; Wei et al., 2015). Importantly, the superior colliculus contains neurons that
68 integrate multisensory stimuli due to synaptic convergence of afferents conveying information from
69 different sensory modalities (Kadunce et al., 2001). These studies established that the effects of MSI
70 are larger when weak or ambiguous stimuli are combined, thus showing an inverse effectiveness
71 relationship with stimulus strength. The underlying hypothesis is that integration of sensory signals
72 from different modalities form a more accurate world percept only if each unisensory signal carries
73 some uncertainty or ambiguity.

74 In goldfish, audiovisual MSI increases the probability and reduces the latency of startle escape
75 behaviors, with an inverse relationship between the MSI effectiveness and the stimulus salience
76 (McIntyre and Preuss, 2019; Martorell and Medan, 2022). These startle escapes (C-starts) are triggered
77 by a pair of reticulospinal neurons (Mauthner cells) that receive visual and auditory inputs through

anatomically segregated pathways. Auditory inputs reach the M-cell lateral dendrite through a disynaptic (2 ms) pathway, while the visual inputs relay information in the optic tectum before reaching the M-cell ventral dendrite through a polysynaptic (20 ms) pathway (Zottoli et al., 1987; Pereda et al., 2004; Korn and Faber, 2005; Szabo et al., 2007). Interestingly, the auditory and visual M-cell dendrites show differences in their cable properties, which appear to be well suited to process inputs from abrupt (i.e. fast raise time) auditory pips and more gradually raising visual looms (Medan et al., 2017). However, it is unclear how auditory and visual signals are integrated at the level of the M-cell to generate a multisensory response.

The accessibility of M-cells for *in vivo* intracellular recordings provides an excellent opportunity to investigate the cellular mechanisms of multisensory integration. Moreover, the one-to-one relationship between a single M-cell action potential and the initiation of a C-start (Zottoli, 1977; Weiss et al., 2006; Zwaka et al., 2022) provides a clear link between behavior and the observed integration in the M-cell. As such, the goal of this study was to reveal the cellular mechanism that underlie the multimodal integration of M-cell initiated startle escapes we observed in the behavioral experiments (McIntyre and Preuss, 2019; Martorell and Medan, 2022). Specifically, we studied how visual and auditory presynaptic pathways and intrinsic membrane properties of the M-cell interact to produce MSI to ultimately enhance threat detection. To this end, we performed intracellular *in vivo* recordings from the M-cell soma using auditory and tectal stimuli with naturalistic dynamics (Preuss et al., 2006; Szabo et al., 2006; Medan et al., 2017). Our results show that the temporal dynamics and strength of stimuli, as well as sensory evoked feed-forward inhibition affect the magnitude of MSI. The results represent a rare characterization of MSI at a single-cell level in a neuron that is sufficient and necessary to trigger a distinct behavior.

102 METHODS

103 **Animals**

104 We used adult goldfish (*Carassius auratus*) of both sexes and 7–10 cm of standard body length. Fish
105 were purchased from Billy Bland Fishery (Taylor, AR, USA), Hunting Creek Fisheries (Thurmont, MD,
106 USA) or Daniel Corriarello Aquarium (Buenos Aires, Argentina) and allowed to acclimate for at least a
107 week after transport. Fish were kept in rectangular Plexiglas holding tanks (30 x 60 x 30 cm^3; 54 l) in
108 groups of up to 10 individuals. Tanks were supplied with filtered and dechlorinated water and
109 maintained at 18 °C. Ambient light was set to a 12-h light/dark photoperiod. Animals were fed floating
110 pellets (Sera, Germany) five times a week. All procedures and protocols were performed in accordance
111 with the guidelines and regulations of the Institutional Animal Care and Use Committee of Hunter
112 College, City University of New York and Facultad de Ciencias Exactas y Naturales, Universidad de
113 Buenos Aires.

114

115 **Auditory stimuli**

116 Abrupt sound stimuli have been extensively used to trigger the short latency escape responses
117 initiated by firing of the M-cell (Eaton et al., 1977; Burgess and Granato, 2007; Neumeister et al., 2008;
118 Weiss et al., 2009; Zheng and Schmid, 2023). Acoustic stimulation produces a complex response in the
119 M-cell which is composed of a fast EPSP superimposed on a depolarizing envelope termed slow EPSP
120 (Szabo et al., 2006). The fast EPSP is composed of fast electrical coupling potentials resulting from
121 firing of the 8th nerve auditory afferences that synapse the distal end of the lateral dendrite of the M-
122 cell (club endings) (Pereda et al., 2004; Szabo et al., 2007). In contrast, the slow EPSP is originated by
123 chemical (glutamatergic) synaptic contacts on the soma and proximal dendrite conveying information
124 from inner hear endorgans and it has been shown that it mostly carries information on stimulus
125 intensity (Szabo et al., 2006). In this study, sound stimuli consisted in single-cycle sound pips (5-ms
126 duration at 200 Hz) produced by a function generator (33210A Agilent Technologies Inc., Santa Clara,

127 CA, USA) connected to a shielded subwoofer (SA-WN250 Sony Corp., Tokyo, Japan) located 30 cm to
128 the right from the recording chamber. Sound stimuli were recorded with a microphone (XM8500,
129 Behringer) positioned 10 cm over the head of the fish. Calibration recordings were performed with a
130 hydrophone (SQ01, Sensor Technology, Ontario, Canada) positioned where the submerged fish was
131 placed during experiments. Since we were interested in studying integration of subthreshold stimuli,
132 we used sound intensities known to be subthreshold for evoking behavioral startle responses
133 (Neumeister et al., 2008; Weiss et al., 2009; Martorell and Medan, 2022). For all experiments we used
134 a sound intensity of 118 dB SPL (relative to 1 μPa in water), except for the experiments in Figure 4
135 where we used a sound intensity of 147 dB SPL (relative to 1 μPa in water). Post-hoc analysis of the
136 M-cell responses in this study revealed that only 3 out of 60 M-cells (5%) fired at least once to an
137 auditory stimulus.
138
139 **Optic tectum stimulation**
140 As shown in other species, goldfish adapt rapidly to repeated natural-looming stimulation (Marquez-
141 Legorreta et al., 2022; Fotowat and Engert, 2023). Indeed, in previous behavioral experiments we
142 presented looming stimuli with intertrial intervals (ITI) of about 4-5 minutes to reduce such adaptation
143 (Preuss et al., 2006; Otero Coronel et al., 2020; Martorell and Medan, 2022). However, ITI of 4-5 min
144 are prohibitively long for steady intracellular recordings. Considering these restrictions, we used tectal
145 stimuli (that bypass the retina) at an ITI of 30 s which does not produce adaptation. We have previously
146 shown that tectal stimulation produce non-adapting synaptic responses that retain key characteristics
147 of looming responses such as fast PSPs riding on top of a ramped depolarization (Preuss et al., 2006;
148 Szabo et al., 2006; Medan and Preuss, 2014; Medan et al., 2017). Tectal stimuli were administered to
149 the mid-anterior rim of the left optic tectum using a bipolar electrode (#30202 FHC, Bowdoin, ME,
150 USA) connected to an isolated stimulator (DS2A; Digitimer Ltd, Welwyn Garden City, UK). In most
151 cases, stimulation [100 µs, 0.1-1mA] in this area was effective in driving subthreshold responses (< 4
152 mV) in the M-cell. To change the strength and dynamics of the tectal stimulation we either used a 60-

153 Hz stimulation train of variable duration (1, 33, 66, 100, 200 ms) or a 100-ms train of variable frequency
154 (1, 33, 100, 200 Hz). We deliberately used tectal stimuli that evoked M-cell firing with a very low
155 probability (6.7%, 4 out of 60 M-cells tested fired at least once to any of the tectal stimuli used).
156
157 **Electrophysiology**

158 M-cell intracellular responses to tectal and acoustic stimuli were studied *in vivo* using standard surgical
159 and electrophysiological recording techniques (Preuss and Faber, 2003; Preuss et al., 2006; Medan et
160 al., 2017). To initiate anesthesia, fish were immersed in 1 liter of ice water with 40 mg/l of the general
161 anesthetic tricaine methanesulfonate (MS-222, Western Chemical, Ferndale, WA, USA), until the fish
162 ceased to swim, lost equilibrium and were unresponsive to a pinch on the tail (typically 10–15 min).
163 They were next treated with 20% benzocaine gel (Ultradent, South Jordan, UT, USA) at incision sites
164 and pin-holding points 5 min prior to surgical procedures. Fish were stabilized in the recording
165 chamber by two pins, one on each side of the head, and ventilated through the mouth with
166 recirculating, aerated saline at 18°C (saline [g/l]: sodium chloride 7.25, potassium chloride 0.38,
167 monosodium phosphate monobasic 0.39, magnesium sulphate 0.11, Hepes 4.77; calcium chloride
168 0.24; dextrose 1.01, pH 7.2). The recording chamber was mounted inside an opaque, thin-walled tank
169 filled with saline that covered the fish up to eye level. The recirculating saline also included a
170 maintenance concentration of the anesthetic MS-222 (20 g/l) that does not interfere with auditory
171 processing (Palmer and Mensinger, 2004; Cordova and Braun, 2007). Next, the spinal cord was
172 exposed with a small lateral incision at the caudal midbody. Bipolar stimulation electrodes were placed
173 on the unopened spinal cord to transmit low-intensity (5–8 V) electrical pulses generated by an
174 isolated stimulator (A 360, WPI, Sarasota, FL, USA). This allowed antidromic activation of the M-cell
175 axons, as confirmed by a visible muscular contraction (twitch). Surgical procedures were performed
176 before a muscle paralysis agent was injected, which allows monitoring the effectiveness of the
177 anesthetic by watching for an increase of opercula movement frequency (largely reduced in deep
178 anesthesia) and movements/twitches in response to the surgical procedures. Shortly before the

179 recordings started, animals were injected I.M. with D-tubocurarine (1 μg g−1 b.w.; Abbott
180 Laboratories, Abbott Park, IL, USA) and a small craniotomy exposed the medulla for
181 electrophysiological recordings. Antidromic stimulation produces a negative potential in the M-cell
182 axon cap (typically 15–20 mV), which unambiguously identifies the axon hillock and allows intracellular
183 recordings from defined locations along the M-cell soma-dendritic membrane (Furshpan and
184 Furukawa, 1962; Furukawa, 1966; Faber and Korn, 1989). Intracellular recordings were acquired using
185 borosilicate glass electrodes (7–10 MΩ) filled with 5 M potassium acetate and an Axoclamp-2B
186 amplifier (Axon Instruments, Foster City, CA, USA) in current-clamp setting. M-cell responses were
187 acquired with a Digidata 1440A (Axon Instruments) at 25 kHz. Electrodes were advanced using
188 motorized micromanipulators (MP-285; Sutter Instruments, Novato, CA, USA) until reaching the axon
189 cap (defined as a site with an extracellular M-cell AP field >10 mV). Next, the electrode was moved 50
190 μm lateral and 50 μm posterior to penetrate the somatic region. Only trials in which the resting
191 membrane potential was between -90 and -70 mV were included in the analysis.
192
193 **Statistical Analyses and Experimental Design**
194 To perform statistical analysis, we used R (version 4.0.2, www.r-project.org) and RStudio (version
195 1.1.456, www. rstudio. com). A significance level of α = 0.05 was used throughout the study. Effects
196 of explanatory variables over response variables were assessed using Linear Models followed by
197 ANOVA or binomial GLMs in the case of binary variables. Paired T-tests were used to compare tectal
198 or auditory responses recorded in left or right M-cells (see Fig. 1). Two tailed Wilcoxon Ranked Sum
199 tests were used for single sample comparisons. Sample size is denoted by N when it refers to the
200 number of goldfish, *n* when it refers to the number of trials (average of 5-10 presentations). In
201 experiments where we recorded from both M-cells of the same animals, results were pooled. Boxplots
202 show the median, 25 and 75th percentile, and lines indicate minimum and maximum values.
203 Postsynaptic responses to acoustic and tectal stimuli were recorded at the M-cell soma and averages
204 of 5-10 responses were used in the statistical analysis. We quantified responses calculating the mean

evoked depolarization in a 12 ms window after sound onset (auditory only trials, A) or after the last tectal stimulus in tectal-only (tectal only trials, T) and multisensory (tectal + auditory trials, M) trials (Fig. 1A-B). We also measured the peak amplitude of the response, which in all cases occurred in the same time window. As peak amplitude analysis produced the same qualitative results, only the mean area analysis is shown.

To characterize the multisensory integration, the responses to M stimuli were normalized to the T and A components. In the field of multisensory integration, multisensory responses are typically normalized to the maximum response of the unisensory stimulus (Meredith and Stein, 1983; Stanford and Stein, 2007; Stein and Stanford, 2008), which we call Multisensory-Maximum Unimodal index (MSI/Max):

$$MSI/Max = M \div max(T, A)$$

The value of this index determines the net effect of the integration, where M is the multisensory response and max(T, A) is the largest of the two unisensory components (all evaluated as the area in a 12-ms window as defined above). Therefore, a *MSI/Max* greater than 1 represents multisensory enhancement, *MSI/Max* lower than 1 represents multisensory inhibition, and *MSI/Max* not significantly different than 1 suggests absence of multisensory integration (Stein and Stanford, 2008). Additionally, to calculate the linearity of the multisensory integration performed by the M-cell, we calculated the ratio between the multisensory response and the sum of the unisensory responses, which we call Multisensory-Sum Unimodals index (MSI/Sum):

$$MSI/Sum = M \div (T + A)$$

The value of this index indicates the linearity of the integration, determined by the ratio of the multisensory response M and the sum of the unisensory components, T and A. MSI/Sum greater than

231 1 representing supralinear integration, MSI/Sum of 1 representing linear integration, and MSI/Sum
232 lower than 1 representing sublinear integration (Stanford et al., 2005).
233 One of the principles that guide multisensory integration is the spatial coherence of the different cues
234 being integrated. If the perceived source localizations of two stimuli overlap, these stimuli are more
235 likely to be integrated. Conversely, if the two stimuli arrive from spatially disparate sources the
236 chances of observing a multisensory integration will decrease (Meredith and Stein, 1996; Stein and
237 Stanford, 2008). The geometrical configuration of the setup in our experiments determined that the
238 loudspeaker used to produce acoustic stimuli was mounted to the right of the fish and electrical
239 stimulation was applied to the left tectum (which normally receives visual signals from the right
240 retina). Whenever possible, we performed recordings from both Mauthner cells. To rule out the
241 possibility of a systematic difference on the responses of either M-cell due to the spatial source of the
242 stimuli, we compared the responses to tectal or auditory stimuli in sequential recordings of the right
243 and left M-cells of the same fish. Supplementary Figure 1 shows representative trace examples for
244 tectal (100 ms 60 Hz tectal train, Fig. Supp. 1A) and auditory (5 ms 200 Hz auditory pip, Fig. Supp. 1B)
245 stimulation from the left (upper traces) or right (lower traces) M-cell of the same fish. The complex
246 post-synaptic potentials were highly stereotypical in successive presentations of a T or A stimuli within
247 and across cells. Analysis from pairs of tectal (Fig. Supp. 1C, N=9) and auditory (Fig. Supp. 1D, N=11)
248 M-cell responses showed no statistical differences between ipsi- and contralateral stimulation (paired
249 T-test, T: $t(8)= 0.18$, $p=0.8573$, A: $t(10)= -0.76$, $p=0.4672$). This confirms previous results indicating that
250 in goldfish, tectal stimulation produces responses with similar latency and amplitude in both M-cells
251 (Zottoli et al., 1987; Canfield, 2006). We therefore pooled data acquired from left or right M-cells for
252 all following analysis.
253
254

255 RESULTS

256

257 **MAUTHNER CELL RESPONSES ARE SENSITIVE TO THE DYNAMICS OF VISUAL TECTAL STIMULI**

258 Multisensory integration is known to be dependent on the saliency of the unimodal components
259 (Stanford et al., 2005; Martorell and Medan, 2022). To create a stimulus set of variable strength and
260 temporal dynamics, we recorded M-cell responses to different electrical trains delivered in the optic
261 tectum.

262 M-cells respond to tectal stimulation with phasic postsynaptic potentials riding on top of a tonic
263 depolarizing response (Figure 1A) that reaches a plateau after 30-100 ms and decays to resting values
264 200-300 ms after the end of the tectal train. To characterize how the M-cell responses depend on the
265 frequency and duration of the stimulation trains in the optical tectum, we recorded responses to 60-
266 Hz trains that varied in duration (Figure 1A-B, N=18), and 100-ms tectal trains that varied in pulse
267 frequency (Figure 1C-D, N=11). The responses to both sets of trains exhibited complex temporal
268 dynamics with a tonic component that progressively builds during the train and a fast phasic
269 component after each pulse (Figure 1A').

270 Increasing the duration of the 60-Hz trains drove stronger tectal responses due to the increase of the
271 tonic component of the response while the phasic response remained unchanged (ANOVA, tonic: $F(3,$
272 $40)=37.29$, $p<0.0001$, phasic: $F(3,40)=0.58$, $p= 0.6311$, Figure 1B). Increasing the frequency of the 100-
273 ms stimulation trains also drove stronger tectal responses due to a large increase in the tonic
274 component (ANOVA, tonic: $F(3, 30)=12.29$, $p<0.0001$). However, increasing the tectal stimulus
275 frequency produced a significant reduction in the amplitude of the phasic component (ANOVA, phasic:
276 $F(3, 30)=11.29$, $p<0.0001$, Figure 1D). Comparing the stimulus trains of variable duration and
277 frequency reveals that modifying the duration of the 60-Hz trains or the frequency of 100-ms trains is
278 similarly effective in tuning the magnitude of the responses. Increasing the duration of a 60 Hz from
279 33 to 200 ms produced a 45% increase in the total response amplitude (phasic + tonic) while increasing

280 the frequency from 30 to 200 Hz produced a 50% increase in the response amplitude (Figures 1 B, D).
281 Since multimodal integration is known to depend on the strength of the unimodal components
282 (Stanford et al., 2005; Martorell and Medan, 2022), in the following multimodal experiments we
283 leveraged this characterization to generate tectal stimuli of variable strength and dynamics. Although
284 both the 60-Hz trains of variable duration and the 100-ms trains of variable frequency evoked
285 responses of similar total amplitude, we decided to include both sets of trains in our multisensory
286 stimuli to determine whether any detected effect depended on the temporal structure of the stimulus
287 or the ratio of phasic-to-tonic responses.

288 **MULTISENSORY ENHANCEMENT IN THE MAUTHNER CELL**

289 Although the M-cell is known to respond to stimuli of different modalities, there are no reports on
290 how it combines and integrates information when two stimuli of different modalities are co-
291 presented. To determine whether multisensory enhancement occurs in the M-cell, we recorded
292 somatic responses to an auditory pip (unisensory auditory, A), a tectal stimulation train (unisensory
293 tectal, T), and their combination (multisensory audiotectal, M) (Figure 2A, E).
294 Increasing the duration of the 60-Hz tectal train positively modulated the multisensory responses
295 (amplitudes ranging from 3.08 ± 0.84 mV to 5.29 ± 1.64 mV, N=17, n=47; LM: evoked depolarization
296 ~ tectal duration, $F(1,45)=17,39$, $p=0.0001$, Figure 2B). We then compared the multisensory responses
297 to their unisensory counterparts. When M responses were normalized to the most effective
298 unisensory response, multisensory stimuli yielded MSI/Max indices that ranged from 1.48 to 1.53 for
299 all stimulus durations (Wilcoxon single sample test mu=1, alternative mu≠1, $p<0.001$ for all stimulus
300 durations, Figure 2C), indicating a significant multisensory enhancement of the response. When the
301 M response was normalized to the sum of both unisensory responses, the MSI/Sum indices were lower
302 than 1 (i.e. sublinear integration, Wilcoxon single sample test mu=1, alternative mu≠1, $p<0.01$) for all
303 cases except for the briefest tectal stimulus, for which the MSI/Sum index was 1.06 (i.e. linear
304 integration, Wilcoxon single sample test mu=1, alternative mu≠1, $p<0.0676$, Figure 2D).

305 Increasing the frequency of a 100-ms tectal train (Figure 2E) was not as effective in modulating the
306 multisensory responses (LM: evoked depolarization ~ tectal frequency, $F(1,39)=3.96$, $p=0.0535$, Figure
307 2F). However, the M responses still exhibited MSI/Max indices that ranged 1.43-1.53 when compared
308 to the largest unimodal stimulus (Figure 2G) indicating that a 100 ms tectal train (irrespective of its
309 frequency) significantly enhances the M-cell response. The MSI/Sum of these M responses ranged
310 0.82 to 0.86 showing a similar sublinear integration to that of the multisensory stimuli with the longer
311 60-Hz trains (Wilcoxon single sample test mu=1, alternative mu≠1, all $p \leq 0.01$, Figure 2H). Neither
312 MSI/Max or MSI/Sum showed a significant dependency with tectal frequency (LM: MSI/Max ~ tectal
313 frequency, $F(1,39)=0.02$, $p=0.882$, MSI/Sum ~ tectal frequency, $F(1,39)=0.49$, $p=0.487$).
314 Overall, these results show that, in all cases, combining an auditory pip with a preceding tectal pulse
315 enhances the M-cell response by about 50%. This multisensory enhancement does not show a strong
316 modulation by the duration or frequency of the tectal stimulus (Figure 2C, G). However, while most
317 multisensory stimuli exhibited a sublinear integration, the multisensory stimulus with the shortest
318 (and weakest) tectal component produced a linear response.
319
320 **TECTAL- AND AUDITORY-EVOKED FEEDFORWARD INHIBITIONS EXHIBIT DISTINCT TEMPORAL**
321 **DYNAMICS**
322
323 Both visual and auditory stimuli evoke feedforward inhibition (FFI) at the perisomatic region of the M-
324 cell through a population of inhibitory interneurons which open chloride channels that produce
325 shunting of the postsynaptic currents (Diamond et al., 1973; Zottoli et al., 1987; Koyama et al., 2011;
326 Tabor et al., 2018). This FFI restricts the temporal window of sensory excitation to terminate the
327 excitatory signal. In combination with passive membrane decay, an increase in FFI will further narrow
328 the window for temporal integration. Conversely, a decrease in FFI would increase the lingering
329 depolarization of a response produced by a previous stimulus, and thus extend the temporal
330 integration window. These differences in the strength or temporal dynamics between visual and

331 auditory evoked FFI may affect multisensory integration (Felch et al., 2016). In the M-cell, auditory or
332 tectal evoked FFI can be quantified as the amplitude reduction of an antidromically evoked "test"
333 action potential (APtest) (Faber and Korn, 1982; Medan et al., 2017). We used a single auditory pip
334 and a brief tectal train as "conditioning" stimuli of similar strength, which evoked comparable peak
335 depolarizations in the M-cell (~5 mV). To test if FFI evoked by auditory or tectal stimuli differed, we
336 evoked the APtest at specific times (2–80 ms) following a sensory stimulus and calculated shunting
337 inhibition as %SI= 100 - APtest/APcontrol ×100, where AP control is the amplitude of the AP without
338 a conditioning stimulus (Figure 3A). Peak FFI inhibition induced by auditory and tectal stimulation
339 showed similar amplitude (Figure 3B, auditory vs. tectal %SI: 13.65 ± 4.74 vs. 14.55 ± 7.50; Kruskal-
340 Wallis chi-squared (1)= 0.01, p = 0.9066, N=19) with peak inhibition at the same time (auditory vs.
341 tectal time (ms) of maximum %SI: 9.04 ± 3.93 vs. 8.85 ± 6.54; Kruskal-Wallis chi-squared(1)= 0.30, p =
342 0.5838, Figure 3C, N=19). In a subset of experiments (N = 7), both auditory and tectal FFI were
343 evaluated sequentially in the same cell and same recording site which allowed us to have an accurate
344 estimate of the inhibition triggered by each sensory modality (Figure 3D). Although the maximum level
345 of inhibition was comparable and was reached in a similar time, recovery from inhibition was much
346 faster for tectal than for auditory FFI. Tectal FFI decayed to 50% of its peak in 8 ms, compared to 30
347 ms for the auditory FFI (Kruskal-Wallis chi-squared (1)= 5.97, p =0.0145, Figure 3E). In addition, the
348 area under the curve for auditory FFI was almost 3 times greater than for tectal FFI (502 vs. 176 %*ms,
349 respectively, Kruskal-Wallis chi-squared (1)= 5.58, p = 0.0181, Figure 3F).
350 These results highlight the key role of the temporal dynamics of the inhibition that reaches the M-cell
351 and which in turn will affect integration in the M-cell. Moreover, these results show that auditory
352 stimuli trigger more prolonged inhibition than tectal stimuli of similar amplitude and decay time. The
353 short-lived FFI that follows tectal stimulation suggests that multiple trains or waves of tectal inputs
354 are more likely to be integrated and summed than multiple sounds. This goes in line with the duration
355 of visual looms that are most effective in triggering the M-cell and eliciting visual C-start escapes
356 (Preuss et al., 2006; Temizer et al., 2015). Differences on the decay rate of inhibition produced by brief

357 tectal or auditory stimuli could affect integration of pairs of brief sensory stimuli depending on their
358 sequence and their timing, which is explored in the next section.
359
360 **STIMULUS TEMPORAL ORDER AND MODALITY AFFECT STIMULI INTEGRATION**
361
362 There are several anatomical and functional differences in the pathways followed by auditory and
363 visual inputs that eventually reach the M-cell soma. First, auditory inputs from the 8th nerve reach the
364 distal lateral dendrite of the M-cell through a disynaptic (≈2 ms) pathway followed by slower inputs
365 from glutamatergic synaptic contacts on the soma and proximal dendrite**.** Visual inputs reach the
366 ventral dendrite after a polysynaptic (≈20 ms) pathway that includes the optical tectum (Zottoli et al.,
367 1987; Szabo et al., 2006). Second, M-cell dendritic characteristics determine modality specific filtering
368 differences resulting in stronger attenuation of visual than auditory signals (Medan et al., 2017). For
369 auditory stimuli, it has been reported that a sound pip that precedes by 20-150 ms a second sound
370 reduces the M-cell response to the second sound, a phenomenon known as auditory prepulse
371 inhibition (Neumeister et al., 2008; Curtin and Preuss, 2015; Tabor et al., 2018). However, it is unclear
372 whether a similar inhibitory integration would hold true for cross-modal and tectal-tectal interactions,
373 since auditory and visual inputs travel through distinct and separated pathways and undergo different
374 filtering.
375 To investigate the role of input modality on M-cell integration we used pairs of similarly brief (~10 ms)
376 auditory pips and tectal pulses 50 ms apart with in all possible sequences, including unisensory
377 combinations (AA, TT) and multisensory combinations (AT, TA, Figure 4, N= 29, n= 50). The amplitude
378 of the tectal stimulation pulse was chosen so that the M-cell responses to the tectal and auditory
379 stimuli were of similar magnitude (4-8 mV). The initial response to the first stimulus (S1, auditory in
380 the example shown in Figure 4A, top trace) decayed passively over the course of 50 ms, and at that
381 point the second stimulus was presented (S2, tectal in the example shown if Figure 4A, bottom trace).
382 The mean lingering depolarization remaining immediately before the second stimulus was delivered

383 (Figure 4A, top trace, pink bar) was slightly larger for the evoked auditory pip than for the tectal
384 stimulus (Figure 4B, A: 1.48 ± 0.79mV vs. T: 0.95 ± 0.50mV, Kruskal-Wallis rank sum test (1) = 5.5173,
385 p = 0.0188).
386 We next calculated the integration indices of the four possible combinations of uni and multisensory
387 pairs (AA, AT, TA, TT). For that, we measured the depolarization in A-only or T-only trials in 12-ms
388 windows. These windows started either 50 ms after stimulus onset to account for the contribution of
389 the first stimulus, S1 (Figure 4A, Resp1, orange area of top trace), or immediately after stimulus
390 presentation to account for the contribution of the second stimulus, S2 (Figure 4A, Resp2, green area
391 of middle trace). Then, we measured the response for pairs of stimuli in a 12-ms window after the
392 presentation of S2 (Figure 4A, Resp(1+2), bottom trace). Finally, we calculated the integration for each
393 type of uni (AA and TT) or multisensory stimuli (AT and TA) defining a "S1-S2 Integration Index" as S1-
394 S2 Int./Sum= Resp(1+2)/(Resp1 + Resp2)). Note that for multisensory trials (i.e. AT or TA), this metric
395 is equivalent to the MSI/Sum index, except for a 50-ms temporal offset in the presentation and
396 quantification of the first stimulus.
397 In the AA trials (N=21) we observed an inhibitory integration (S1-S2 Int./Sum < 1, two-sided Wilcoxon
398 rank test, p<0.0001) with the first auditory pip reducing the amplitude expected for the second pip by
399 42%, as others have previously described (Neumeister et al., 2008; Curtin and Preuss, 2015; Tabor et
400 al., 2018). The AT combination also showed sublinear integration (S1-S2 Int./Sum < 1, two-sided
401 Wilcoxon rank test, p = 0.0078) while the TT and TA combinations showed linear integration (S1-S2
402 Int./Sum =1, two-sided Wilcoxon rank test, VA: p = 0.0681, VV: p = 0.9453, Figure 4C). The inhibitory
403 effect in the AA combination was significantly larger than for the AT combination (Figure 4C, 1w-
404 ANOVA, F=38.34, p<0.0001).
405
406 **MULTISENSORY INTEGRATION IN THE MAUTHNER CELL SHOWS INVERSE EFFECTIVENESS**
407

408 The principle of inverse effectiveness states that the effects of multisensory integration are typically
409 larger when the components of a multisensory stimulus are weak. Throughout our experiments, we
410 only observed linear integration of multisensory stimuli when presenting single tectal pulses (Figure
411 2C, 1ms tectal), or brief (~10 ms) trains (Figure 4, AT – TA), and observed sublinear integration for
412 multimodal stimuli with longer tectal trains (Figure 2D-H). However, these results represent the
413 average MSI for each group for a specific set of experimental conditions and effectively simplify the
414 diverse range of responses across trials, experimental conditions, and fish. To compare the overall
415 dependence of the multisensory enhancement on the strength of sensory inputs, we pooled the
416 multisensory integration indexes for experiments irrespective of sequence of stimuli (AT and TA, N=18,
417 n=174), tectal train duration (from a single 1-ms tectal pulse to a 200-ms train) and frequency (from a
418 single pulse to 1000Hz) (Figure 5A, MSI/Max and B, MSI/Sum). We found a significant inverse
419 correlation between the magnitude of the multisensory enhancement and the magnitude of the
420 unisensory components (MSI/Max, LM, $F(1,172)$: 28.17, $p<0.0001$; MSI/Sum, LM, $F(1,172)$: 67.33,
421 $p<0.0001$). This result parallels the inverse effectiveness reported at the behavioral level in goldfish
422 (McIntyre and Preuss, 2019; Martorell and Medan, 2022), confirming that the relative multisensory
423 enhancement obtained by combining two inputs is proportionally higher when the stimuli are weak.
424 Combinations of weak stimuli (<2.5mV, Figure 5B) produce supralinear multisensory responses that
425 are between 50-100% stronger than the most effective unisensory stimulus (Figure 5A). Noteworthy,
426 these results provide robust evidence that in the escape network of fish, inverse effectiveness of
427 multisensory integration is implemented, at least, at the single (Mauthner) cell level.
428 Although the previous analysis was based on subthreshold responses, in a low proportion of
429 experiments M-cells fired in response to sensory stimulation. Of 60 M-cells tested, 3 (5%) fired to
430 auditory, 4 (6.7%) to tectal, and 7 (11.7%) to multimodal stimuli. Although firing was observed in a
431 very limited number of cells, these data show a tendency to a higher response probability to
432 multisensory than unisensory stimuli that did not reach statistical significance (Pearson's chi-squared
433 test $X2$: 0.40, $p=0.5269$). Figure 5C shows two examples from two different animals in which the M-

434 cells showed subthreshold responses to unisensory stimuli and elicited an action potential when the
435 two stimuli are combined. Since an action potential in the M-cell triggers the initiation of a C-start
436 escape, these are examples of behaviors that only occurred in response to a multisensory stimulus but
437 not to either of the unisensory components. This highlights how, because of the all-or-nothing nature
438 of action potentials, relatively small increments in the M-cell response due to multisensory
439 enhancement could be sufficient to make the cell trigger and have a profound effect in escape
440 behavior, even if the integration is sublinear.
441

DISCUSSION

The Mauthner-cell system triggers a behavior of vital importance: escaping from predators. A combination of fast afferent circuits, synaptic specialization, special intrinsic properties and topology of the M-cell contribute in concert to a fast startle escape response (Eaton et al., 1991; Korn and Faber, 2005). Here we show that the M-cell incorporates multisensory information to enhance its responses and characterize how the integration of multiple stimuli is affected by the modality, spatial source, temporal structure, temporal order, and intensity of the stimuli. Although multisensory enhancement has been previously described in different neural populations and across a wide range of species, it was unclear whether the activity of these neurons was necessary, sufficient, or even influenced the execution of behavioral responses to multisensory stimuli. In contrast to other known multisensory structures of vertebrates multisensory integration in the M-cell has an unequivocal function in fish behavior and survival, as it directly determines whether and when a C-start is triggered (McIntyre and Preuss, 2019; Martorell and Medan, 2022) .

Different factors differentially affect the summation and integration of auditory and visual inputs to the M-cell. First, sensory inputs are subject to different passive decays depending on the site of the dendritic arbor at which they arrive. Auditory inputs reach the M-cell distal lateral dendrite through dense mixed electrical and chemical synapses driven through the posterior 8th-nerve afferents and the proximal dendrite through indirect glutamatergic inputs conveying information from inner ear endorgans (Szabo et al., 2006, 2007). In contrast, visual inputs arriving to the ventral dendrite establish synapses that do not show additional specializations as the club endings (Zottoli et al., 1987; Cachope et al., 2007; Szabo et al., 2007). Second, the geometrical properties of the M-cell lateral and ventral dendrites (length and tapering) impose different filters on the input signal which determine a stronger spatial decay for visual than for auditory signals (Medan et al., 2017). Third, as excitatory signals reach the soma, the active ion conductances decrease the membrane resistance and impact the response to following signals (Hodgkin, 1947). Finally, the magnitude and dynamics of the stimuli will also affect integration. Both abrupt auditory pips and longer lasting auditory looms generate fast EPSPs that

468 depend on the stimulus frequency and a depolarizing envelope proportional to the stimulus amplitude
469 (Szabo et al., 2006) that slowly decays to baseline (Figure 4). Although the pathways for auditory and
470 visual inputs are completely different, tectal responses also consist of fast peaks that track stimulus
471 frequency and a tonic depolarizing envelope proportional both to stimulus duration and frequency
472 (Figure 1) that also decays slowly (Figure 4).
473 These temporal dynamics of the responses modulate the effective multisensory integration in the M-
474 cell soma, which emerges as a complex, nonlinear interaction between "positive" (input strength and
475 summation) and "negative" (temporal and spatial decay, feedforward inhibition, and depolarization-
476 induced decrease in input resistance) contributions. These factors likely influence integration in any
477 multisensory neuron. However, the accumulated knowledge on the presynaptic pathways and the
478 intrinsic mechanisms operating in the M-cell combined with its functional role in commanding the
479 initiation of the C-start response makes this neuron a unique model for analyzing multisensory
480 integration in a single identifiable neuron.
481 We have previously shown that fish exhibit a behavioral multisensory enhancement of the C-start
482 escape response for audiovisual stimuli, and that this effect is reduced when increasing the salience
483 of the unisensory stimuli (Martorell and Medan, 2022). Therefore, one of our goals here was to
484 investigate if the inverse effectiveness principle observed behaviorally had its correlation in
485 integration processes taking place in the M-cell. Paralleling our previous behavioral results, here we
486 show through intracellular recordings that the response evoked by an auditory pip can be increased
487 by about 50% when it is preceded by a tectal stimulus (Figure 2C, G). This enhancement was not
488 affected by relatively large changes in stimulus frequency. The plateau in the tonic depolarization
489 observed 30-50 ms after a sustained stimulus (Figure 1A) combined with the low-pass filtering
490 properties of the membrane could be responsible for the lack of frequency effects. These two
491 mechanisms point to the M-cell role as a "sudden" stimulus detector rather than a precise coder of
492 sensory stimulus properties.

493 When we combined a tectal train with an auditory pip to obtain a multisensory stimulus, the response
494 was smaller than the sum of the evoked depolarization of the two components (Figures 2D, H). This
495 sublinear effect was expected in the case of passive integration, since cellular biophysics predict a
496 sublinear integration of subthreshold inputs due to a reduction in the driving force of sodium and the
497 aperture of ion channels that reduce the membrane resistance. Noteworthy, action potentials are all-
498 or-nothing events, so the effects when the membrane potential is close to the threshold, sublinear
499 summation can determine that an otherwise silent neuron fires an AP (Figure 5C). Therefore, a weak
500 (subthreshold) auditory pip combined by a weak visual stimulus in close temporal association might
501 be sufficient for triggering an escape response. Indeed, analysis of 60 M-cells tested with A, T and M
502 stimuli showed that auditory stimuli evoked firing in 5% of cells, tectal stimuli in 6.7% of cells but
503 almost 12% of M-cells fired in response to multisensory stimuli. Even though these results might be
504 affected by anesthesia and paralyzing agents they provide a mechanistic support to our previous
505 behavioral observations (Martorell and Medan, 2022).
506 Importantly, for the weakest multisensory stimuli the M-cell response deviated from this sublinear
507 integration (Figures 2C and 5A). When the sum of unisensory components is less than 2.5 mV
508 (essentially a single tectal stimulus immediately followed by a single auditory pip) summation is linear
509 (Figure 2D and 5A). This suggests the existence of one or more active mechanism/s of multisensory
510 integration upstream of the M-cell soma, potentially through a presynaptic neuron that also receives
511 audiovisual inputs and projects to the M-cell or locally at the level of the dendritic tree of the M-cell.
512 Moreover, M-cell membrane non-linearities in the lateral and ventral dendrites which progressively
513 increase M-cell excitability for depolarizations above 5 mV have been described previously (Faber and
514 Korn, 1986; Medan et al., 2017). Such nonlinear properties might enhance multisensory integration of
515 weak stimuli (Martorell and Medan, 2022) providing a cellular mechanism for the principle of inverse
516 effectiveness of multisensory integration.
517 The temporal structure of the multisensory stimuli is crucial to allow the animal to effectively “bind”
518 or associate both signals as coming from a single source (Stein and Stanford, 2008). In the M-cell, this

519 translates into the time window where the effect on the membrane voltage (excitatory or inhibitory)
520 persists. Here, we found that a delay of 50 ms between the components of a low-amplitude
521 multisensory stimuli result in a linear summation of the signals (Figure 4C) and that the temporal order
522 of the components produces a slight effect in the integration (Figure 4C, AT vs. TA) (Felch et al., 2016).
523 As it has been previously suggested, the lengthy decay of the slow EPSP of the auditory pip (or the
524 tonic component of the tectal train) probably contributed to relax the requirement for coincident
525 inputs, effectively broadening the temporal window of integration (Szabo et al., 2006). On the other
526 hand, the integration of unisensory stimuli was dependent on the modality of the stimuli: two tectal
527 (TT) stimuli summed linearly while two auditory (AA) stimuli summed sublinearly (Figure 4C). This
528 difference might be due to differences in both the presynaptic networks that mediate PPI (Tabor et
529 al., 2018) and in the temporal decay of auditory and tectally evoked FFI (Figure 3D). Auditory stimuli
530 produce a longer-lasting inhibition than tectal stimuli of similar strength (Figure 3F) and while tectal
531 inhibition is almost extinct 50 ms after a tectal stimulus, auditory inhibition stabilizes at around 50%
532 of the maximum inhibitory effect in a time window of 30 to 70 ms after an auditory stimulus (Figure
533 3E). Interestingly, the integration of AT stimuli was smaller than that of TA, supporting a differential
534 cross-modal and intra-modal integration of the excitatory or inhibitory components (Figure 4C).
535 Another factor that could be contributing to the differential integration between AA and AT stimuli is
536 that FFI inhibition is likely to be heterogeneously spread in the perisomatic area around the M-cell. If
537 auditory stimulation recruits inhibitory PHP neurons that target the proximal lateral dendrite of the
538 M-cell, a subsequent sensory input propagating along the lateral dendrite (i.e, auditory input) would
539 suffer stronger attenuation than one reaching the soma through the ventral dendrite (i.e., tectal
540 input). However, specific studies are required to test this hypothesis as it is still unclear if auditory and
541 tectal afferent fibers synapse the same or different sets of inhibitory neurons and which is the spatial
542 distribution of those inhibitory contacts. Additionally, presynaptic effects could also contribute to the
543 asymmetry in unimodal auditory (AA) vs. unimodal tectal (TT) or multisensory processing. A subset of
544 glutamatergic Gsx1 neurons located in rhombomere 4 have been shown to mediate M-cell auditory

presynaptic inhibition (Tabor et al., 2018). These neurons produce presynaptic inhibition of 8th nerve auditory fibers adjacent to the distal portion of the M-cell lateral dendrite but leave unaffected the ventral dendrite. This mechanism could therefore affect the processing of pairs of sensory signals that initiate with an auditory component (AA, AT) and leave the integration of tectal or multisensory stimuli unaffected.

AUTHOR CONTRIBUTIONS

SOC, TP and VM conceived the research. SOC and VM performed experiments and analyzed the data. SOC and VM wrote the manuscript.

558 **References**

559 Burgess HA, Granato M (2007) Sensorimotor gating in larval zebrafish. J Neurosci 27:4984–4994.

560 Cachope R, Mackie K, Triller A, O'Brien J, Pereda AE (2007) Potentiation of electrical and chemical
561 synaptic transmission mediated by endocannabinoids. Neuron 56:1034–1047.

562 Canfield JG (2006) Functional evidence for visuospatial coding in the Mauthner neuron. Brain Behav
563 Evol 67:188–202.

564 Cordova MS, Braun CB (2007) The use of anesthesia during evoked potential audiometry in goldfish
565 (Carassius auratus). Brain Res 1153:78–83.

566 Curtin PCP, Preuss T (2015) Glycine and GABAA receptors mediate tonic and phasic inhibitory
567 processes that contribute to prepulse inhibition in the goldfish startle network. Front Neural Circuits
568 9:12.

569 Dean P, Redgrave P, Westby GWM (1989) Event or emergency? Two response systems in the
570 mammalian superior colliculus. Trends Neurosci 12:137–147.

571 Diamond J, Roper S, Yasargil GM (1973) The membrane effects, and sensitivity to strychnine, of
572 neural inhibition of the Mauthner cell, and its inhibition by glycine and GABA. J Physiol 232:87–111.

573 Eaton RC, Bombardieri RA, Meyer DL (1977) The Mauthner-initiated startle response in teleost fish. J
574 Exp Biol 66:65–81.

575 Eaton RC, DiDomenico R, Nissanov J (1991) Role of the Mauthner cell in sensorimotor integration by
576 the brain stem escape network. Brain Behav Evol 37:272–285.

577 Faber DS, Korn H (1982) Transmission at a central inhibitory synapse. I. Magnitude of unitary
578 postsynaptic conductance change and kinetics of channel activation. J Neurophysiol 48:654–678.

579 Faber DS, Korn H (1986) Instantaneous inward rectification in the Mauthner cell: a postsynaptic
580 booster for excitatory inputs. Neuroscience 19:1037–1043.

581 Faber DS, Korn H (1989) Electrical field effects: their relevance in central neural networks. Physiol
582 Rev 69:821–863.

583 Felch DL, Khakhalin AS, Aizenman CD (2016) Multisensory integration in the developing tectum is
584 constrained by the balance of excitation and inhibition. eLife 5:e15600.

585 Fotowat H, Engert F (2023) Neural circuits underlying habituation of visually evoked escape
586 behaviors in larval zebrafish Kawakami K, Moore T, eds. eLife 12:e82916.

587 Furshpan EJ, Furukawa T (1962) Intracellular and extracellular responses of the several regions of the
588 Mauthner cell of the goldfish. J Neurophysiol 25:732–771.

589 Furukawa T (1966) Synaptic interaction at the mauthner cell of goldfish. Prog Brain Res 21:44–70.

590 Gil-Guevara O, Bernal HA, Riveros AJ (2022) Honey bees respond to multimodal stimuli following the
591 principle of inverse effectiveness. J Exp Biol 225:jeb243832.

592 Hodgkin AL (1947) The membrane resistance of a non-medullated nerve fibre. J Physiol 106:305–
593 318.

Kadunce DC, Vaughan JW, Wallace MT, Stein BE (2001) The influence of visual and auditory receptive field organization on multisensory integration in the superior colliculus. Exp Brain Res 139:303–310.

Korn H, Faber DS (2005) The Mauthner cell half a century later: a neurobiological model for decision-making? Neuron 47:13–28.

Koyama M, Kinkhabwala A, Satou C, Higashijima S, Fetcho J (2011) Mapping a sensory-motor network onto a structural and functional ground plan in the hindbrain. Proc Natl Acad Sci U S A 108:1170–1175.

Marquez-Legorreta E, Constantin L, Piber M, Favre-Bulle IA, Taylor MA, Blevins AS, Giacomotto J, Bassett DS, Vanwalleghem GC, Scott EK (2022) Brain-wide visual habituation networks in wild type and fmr1 zebrafish. Nat Commun 13:895.

Martorell N, Medan V (2022) Audiovisual integration in the Mauthner cell enhances escape probability and reduces response latency. Sci Rep 12:1097.

McIntyre C, Preuss T (2019) Influence of Stimulus Intensity on Multimodal Integration in the Startle Escape System of Goldfish. Front Neural Circuits 13:7.

Medan V, Mäki-Marttunen T, Sztarker J, Preuss T (2017) Differential processing in modality-specific Mauthner cell dendrites. J Physiol.

Medan V, Preuss T (2014) The Mauthner-cell circuit of fish as a model system for startle plasticity. J Physiol-Paris 108:129–140.

Meredith MA, Stein BE (1983) Interactions among converging sensory inputs in the superior colliculus. Science 221:389–391.

Meredith MA, Stein BE (1996) Spatial determinants of multisensory integration in cat superior colliculus neurons. J Neurophysiol 75:1843–1857.

Metaxakis A, Petratou D, Tavernarakis N (2018) Multimodal sensory processing in Caenorhabditis elegans. Open Biol 8:180049.

Neumeister H, Szabo TM, Preuss T (2008) Behavioral and physiological characterization of sensorimotor gating in the goldfish startle response. J Neurophysiol 99:1493–1502.

Otero Coronel S, Martorell N, Beron de Astrada M, Medan V (2020) Stimulus Contrast Information Modulates Sensorimotor Decision Making in Goldfish. Front Neural Circuits 14:23.

Palmer LM, Mensinger AF (2004) Effect of the anesthetic tricaine (MS-222) on nerve activity in the anterior lateral line of the oyster toadfish, Opsanus tau. J Neurophysiol 92:1034–1041.

Pereda AE, Rash JE, Nagy JI, Bennett MVL (2004) Dynamics of electrical transmission at club endings on the Mauthner cells. Brain Res Brain Res Rev 47:227–244.

Preuss T, Faber DS (2003) Central cellular mechanisms underlying temperature-dependent changes in the goldfish startle-escape behavior. J Neurosci 23:5617–5626.

Preuss T, Osei-Bonsu PE, Weiss SA, Wang C, Faber DS (2006) Neural representation of object approach in a decision-making motor circuit. J Neurosci Off J Soc Neurosci 26:3454–3464.

Rowland BA, Quessy S, Stanford TR, Stein BE (2007) Multisensory integration shortens physiological response latencies. J Neurosci Off J Soc Neurosci 27:5879–5884.

632 Stanford TR, Quessy S, Stein BE (2005) Evaluating the Operations Underlying Multisensory
633 Integration in the Cat Superior Colliculus. J Neurosci 25:6499–6508.

634 Stanford TR, Stein BE (2007) Superadditivity in multisensory integration: putting the computation in
635 context. Neuroreport 18:787–792.

636 Stein BE, Stanford TR (2008) Multisensory integration: current issues from the perspective of the
637 single neuron. Nat Rev Neurosci 9:255–266.

638 Szabo TM, McCormick CA, Faber DS (2007) Otolith endorgan input to the Mauthner neuron in the
639 goldfish. J Comp Neurol 505:511–525.

640 Szabo TM, Weiss SA, Faber DS, Preuss T (2006) Representation of auditory signals in the M-cell: role
641 of electrical synapses. J Neurophysiol 95:2617–2629.

642 Tabor KM, Smith TS, Brown M, Bergeron SA, Briggman KL, Burgess HA (2018) Presynaptic Inhibition
643 Selectively Gates Auditory Transmission to the Brainstem Startle Circuit. Curr Biol CB 28:2527-
644 2535.e8.

645 Temizer I, Donovan JC, Baier H, Semmelhack JL (2015) A Visual Pathway for Looming-Evoked Escape
646 in Larval Zebrafish. Curr Biol CB 25:1823–1834.

647 Wallace MT, Meredith MA, Stein BE (1998) Multisensory integration in the superior colliculus of the
648 alert cat. J Neurophysiol 80:1006–1010.

649 Wei P, Liu N, Zhang Z, Liu X, Tang Y, He X, Wu B, Zhou Z, Liu Y, Li J, Zhang Y, Zhou X, Xu L, Chen L, Bi G,
650 Hu X, Xu F, Wang L (2015) Processing of visually evoked innate fear by a non-canonical thalamic
651 pathway. Nat Commun 6:6756.

652 Weiss SA, Preuss T, Faber DS (2009) Phase encoding in the Mauthner system: implications in left-
653 right sound source discrimination. J Neurosci 29:3431–3441.

654 Weiss SA, Zottoli SJ, Do SC, Faber DS, Preuss T (2006) Correlation of C-start behaviors with neural
655 activity recorded from the hindbrain in free-swimming goldfish (Carassius auratus). J Exp Biol
656 209:4788–4801.

657 Zheng A, Schmid S (2023) A review of the neural basis underlying the acoustic startle response with a
658 focus on recent developments in mammals. Neurosci Biobehav Rev 148:105129.

659 Zhou G, Lane G, Noto T, Arabkheradmand G, Gottfried JA, Schuele SU, Rosenow JM, Olofsson JK,
660 Wilson DA, Zelano C (2019) Human olfactory-auditory integration requires phase synchrony between
661 sensory cortices. Nat Commun 10:1168.

662 Zottoli SJ (1977) Correlation of the startle reflex and Mauthner cell auditory responses in
663 unrestrained goldfish. J Exp Biol 66:243–254.

664 Zottoli SJ, Hordes AR, Faber DS (1987) Localization of optic tectal input to the ventral dendrite of the
665 goldfish Mauthner cell. Brain Res 401:113–121.

666 Zwaka H, McGinnis OJ, Pflitsch P, Prabha S, Mansinghka V, Engert F, Bolton AD (2022) Visual object
667 detection biases escape trajectories following acoustic startle in larval zebrafish. Curr Biol 32:5116-
668 5125.e3.

669

670

671 FIGURE LEGENDS

672 **Figure 1**. M-cell responses to tectal stimulation. A. M-cell responses to a 60 Hz tectal train of 200 ms
673 were used to measure the evoked depolarization at 1, 33, 100 and 200 ms after stimulus onset during
674 a 12-ms time window (colored vertical boxes). A´. Lower inset. Black and grey bars in the trace show
675 amplitudes of the tonic and phasic components of the response, respectively. The horizontal dotted
676 line indicates the baseline for quantification of each component. B. Mean amplitude (± SEM) of the
677 phasic (shaded) and tonic (solid) components of tectal trains for the time windows described in A. C.
678 M-cell responses to a 100 ms tectal pulse train of 30, 60, 100 or 200 Hz were recorded and quantified
679 as in A, at the end of the pulse. D. Mean amplitude (± SEM) of the phasic (shaded) and tonic (solid)
680 components of 100-ms tectal trains of different frequency.

681

682 **Figure 2**. Multisensory integration in the M-cell. A. Diagram of stimulation (left) and response
683 examples (right). The response examples correspond, to a single acoustic pulse (blue trace) and to
684 their multisensory combination (purple). Below the traces diagram of the stimulation is shown in gray.
685 B. Stacked bars comparing mean (± SEM) depolarization evoked by tectal trains of indicated duration
686 (T, orange), auditory (A, blue) or their multisensory combination (purple). C. Boxplots showing the
687 ratios between the multisensory responses and the maximum unisensory response (MSI/Max). D.
688 Boxplots showing the ratios between the multisensory responses and the sum of its unisensory
689 components (MSI/Sum). E-H. As in A-D but for 100 ms tectal trains of different frequencies.

690

691 **Figure 3**. Auditory and tectal FFI have different decay dynamics. A. Diagram of auditory or tectal
692 feedforward inhibition circuits (center), and the quantification of sensory evoked shunting inhibition
693 as a reduction of M-cell AP amplitude (left, auditory: shaded-blue area; right, tectal: shaded-red area)
694 to a control AP (black trace). B-C. Boxplots of peak inhibition and time of peak inhibition triggered by
695 acoustic or tectal stimuli. D. Mean (±SEM) FFI triggered by tectal and auditory inputs measured in the
696 same M-cells at different time points between 0 and 70 ms post-stimulus. E. Boxplot of the time

elapsed to 50% decay of peak FFI for the auditory (left) and tectal (right) stimuli. *p=0.0145. F. Area below the curve (0-70 ms) for the auditory (left) and tectal (right) stimuli. *p=0.0181.

Figure 4. Effect of stimulus sequence and modality on M-cell integration. A. Representative responses of one M-cell to two stimuli presented either in different trials, or in the same trials with a 50 ms offset. Schematics below each trace the order of stimuli and the area where responses were quantified. The pink bar indicates the time point at which the lingering depolarization of the first response was measured. Note that this analysis was performed for trials in which Stim1 and Stim2 could be either A or T, resulting in trials AA, TT, TA and AT sequences. B. Lingering depolarization after 50 ms of a single auditory pip or a short tectal train. *p=0.0188. C. Integration in the M-cell for pairs of uni- or multisensory stimuli with a 50 ms delay was calculated as the ratio: Resp (1+2) / (Resp1 + Resp2).

Figure 5. Multisensory integration of subthreshold unisensory stimuli. A. MSI/Max vs. the maximum unisensory response of different multisensory stimuli, irrespective of duration, frequency, or sequence of stimulation. B. Similar to A, but with the MSI/Sum instead vs. the sum of the unisensory responses. C. Example traces in which the integration of subthreshold unisensory tectal (T, red) and auditory (A, blue) stimuli evokes an M-cell AP (TA, purple). Responses to an auditory pip only triggered an action potential when they were preceded by four tectal pulses delivered at 333Hz (left) or a 200-ms tectal train at 60Hz (right).

Supplementary Figure 1. A-B. Representative recordings of left or right M-cell somatic responses to an electric stimulus train delivered to the left tectum (A) or to a short 200 Hz sound pip produced by a loudspeaker placed to the right side of the fish (B). The mean (of 3-5 repetitions) response is shown in solid color and the diagram of the tectal stimulus or the the sound pip are shown below the traces. Dashed boxes indicate the 12-ms time windows following the stimulus where the responses were

723 quantified. C-D. Boxplots showing the median, upper and lower quartiles and comparing the response
724 to the same stimulus in the left or right M-cell in 9 fish for the tectal stimulus (C) and 11 fish for the
725 auditory stimulus (D). Markers with the same color in left and right belong to pairs of M-cells of the
726 same fish. No differences were found in the evoked response amplitude between the left and right M-
727 cells or for tectal or auditory stimuli.
728

Figure 1

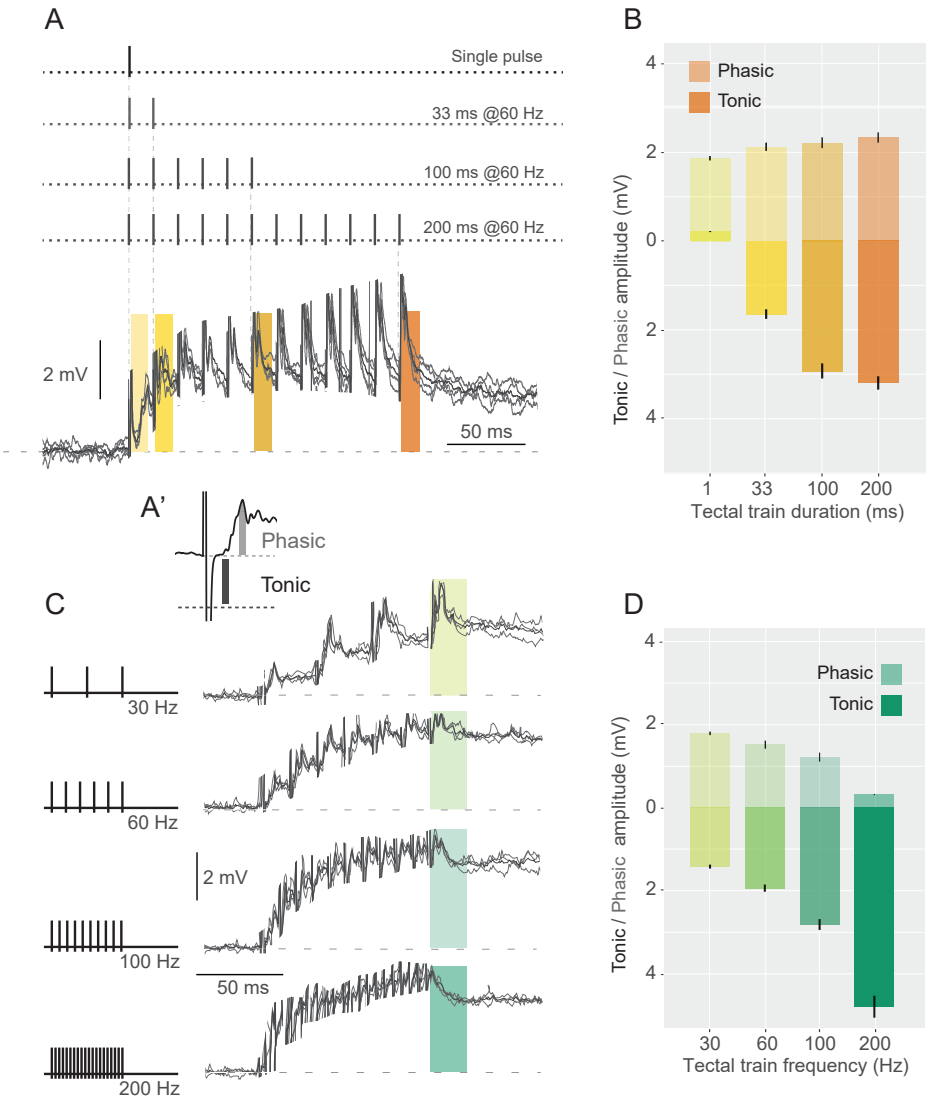
A
Single pulse
33 ms @60 Hz
100 ms @60 Hz
200 ms @60 Hz
2 mV
50 ms
A'
Phasic
Tonic
B
Phasic
Tonic
Tonic / Phasic amplitude (mV)
4
2
0
2
4
1
33
100
200
Tectal train duration (ms)
C
30 Hz
60 Hz
100 Hz
200 Hz
2 mV
50 ms
D
Phasic
Tonic
Tonic / Phasic amplitude (mV)
4
2
0
2
4
30
60
100
200
Tectal train frequency (Hz)

Figure 2

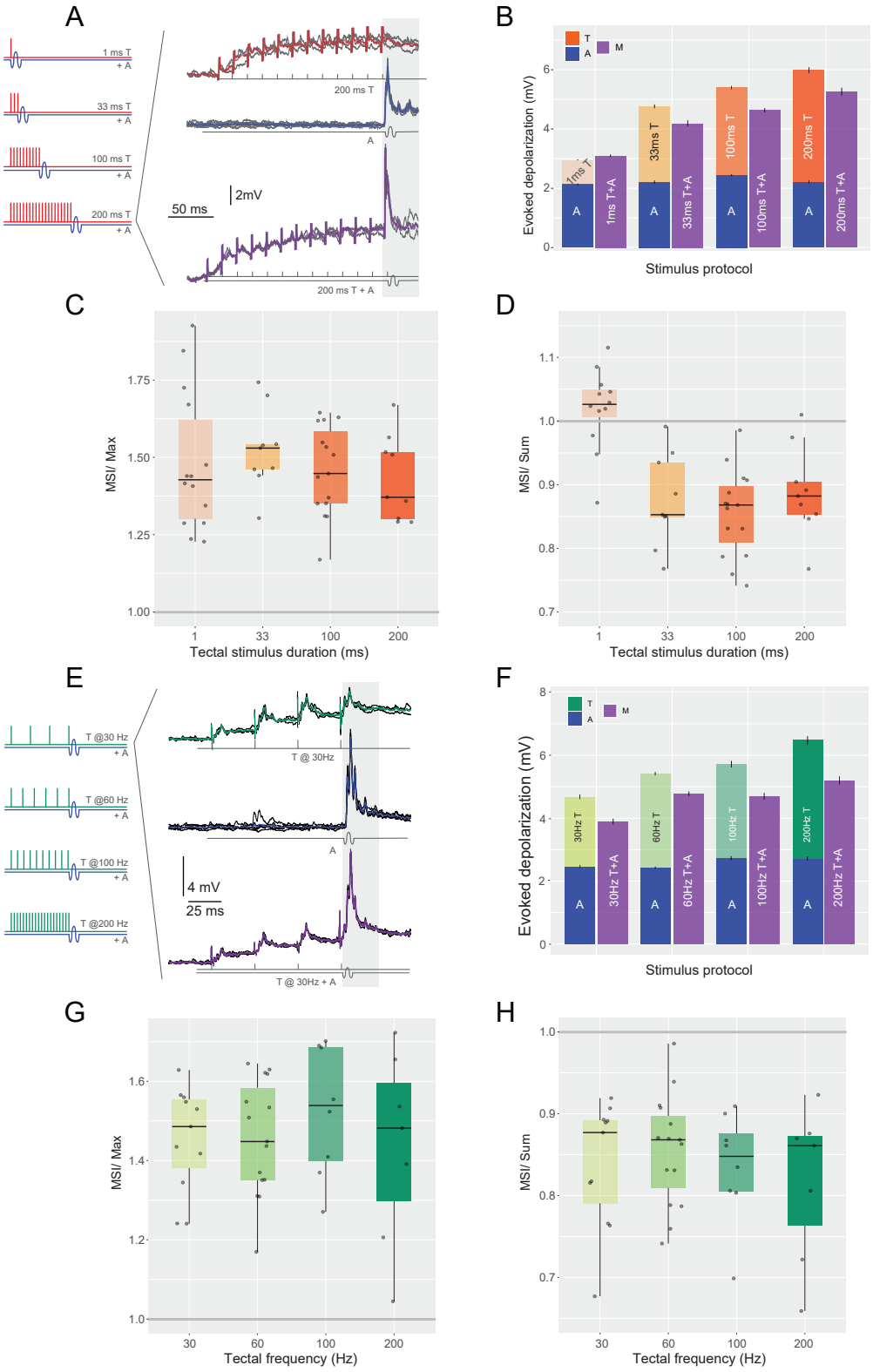
A
1 ms T
+ A
33 ms T
+ A
100 ms T
+ A
200 ms T
+ A
200 ms T
A
2mV
50 ms
200 ms T + A
B
T
A
M
Evoked depolarization (mV)
1ms T
1ms T+A
33ms T
33ms T+A
100ms T
100ms T+A
200ms T
200ms T+A
Stimulus protocol
C
MSI/ Max
Tectal stimulus duration (ms)
D
MSI/ Sum
Tectal stimulus duration (ms)
E
T @30 Hz
+ A
T @60 Hz
+ A
T @100 Hz
+ A
T @200 Hz
+ A
T @ 30Hz
A
4 mV
25 ms
T @ 30Hz + A
F
T
A
M
Evoked depolarization (mV)
30Hz T
30Hz T+A
60Hz T
60Hz T+A
100Hz T
100Hz T+A
200Hz T
200Hz T+A
Stimulus protocol
G
MSI/ Max
Tectal frequency (Hz)
H
MSI/ Sum
Tectal frequency (Hz)

Figure 3

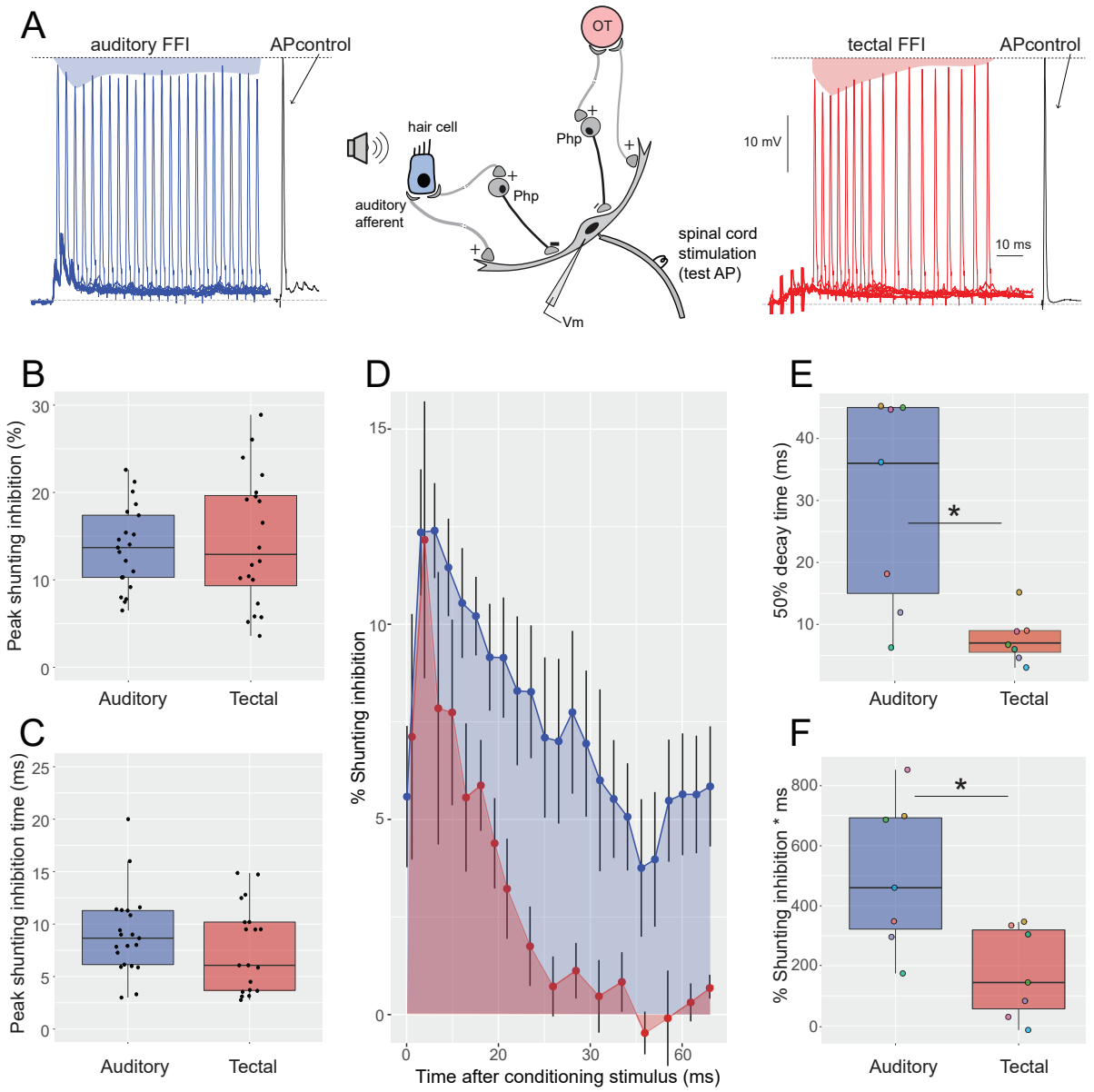
A
auditory FFI
APcontrol
hair cell
auditory afferent
Php
Php
OT
spinal cord stimulation (test AP)
Vm
tectal FFI
APcontrol
10 mV
10 ms
B
Peak shunting inhibition (%)
Auditory
Tectal
C
Peak shunting inhibition time (ms)
Auditory
Tectal
D
% Shunting inhibition
Time after conditioning stimulus (ms)
E
50% decay time (ms)
*
Auditory
Tectal
F
% Shunting inhibition * ms
*
Auditory
Tectal

Figure 4

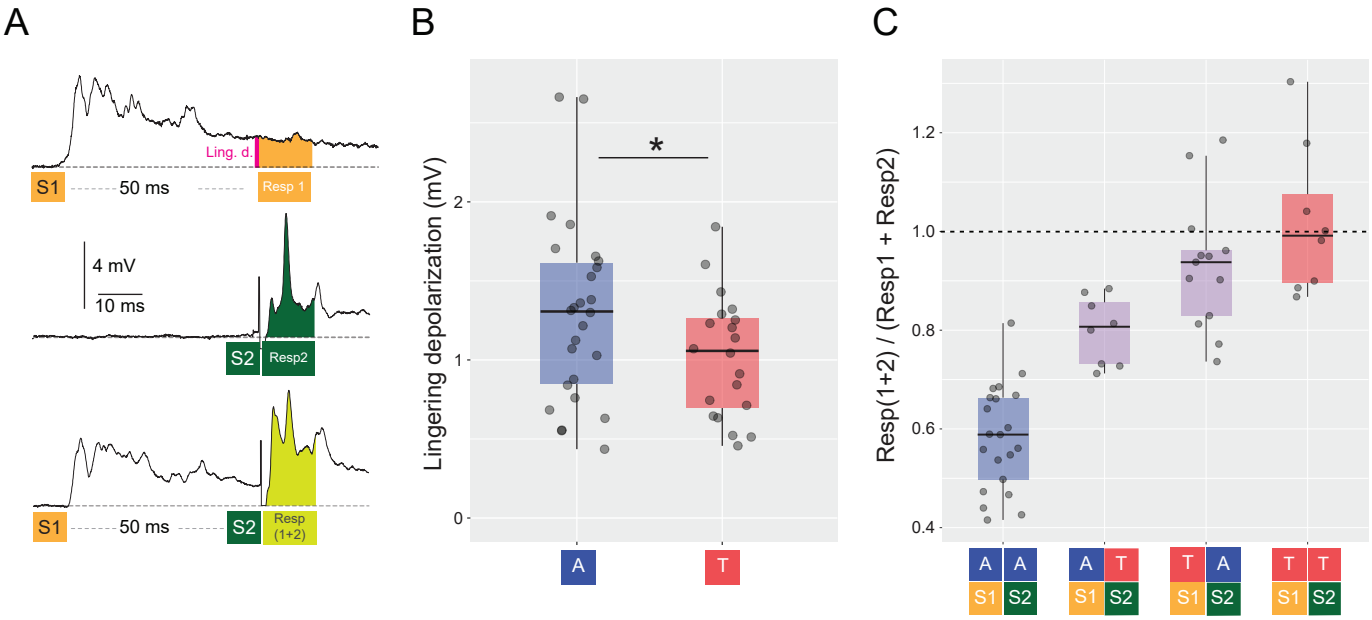
A
Ling. d.
S1
50 ms
Resp 1
4 mV
10 ms
S2
Resp2
S1
50 ms
S2
Resp
(1+2)
B
Lingering depolarization (mV)
*
A
T
C
Resp(1+2) / (Resp1 + Resp2)
A A
S1 S2
A T
S1 S2
T A
S1 S2
T T
S1 S2

Figure 5

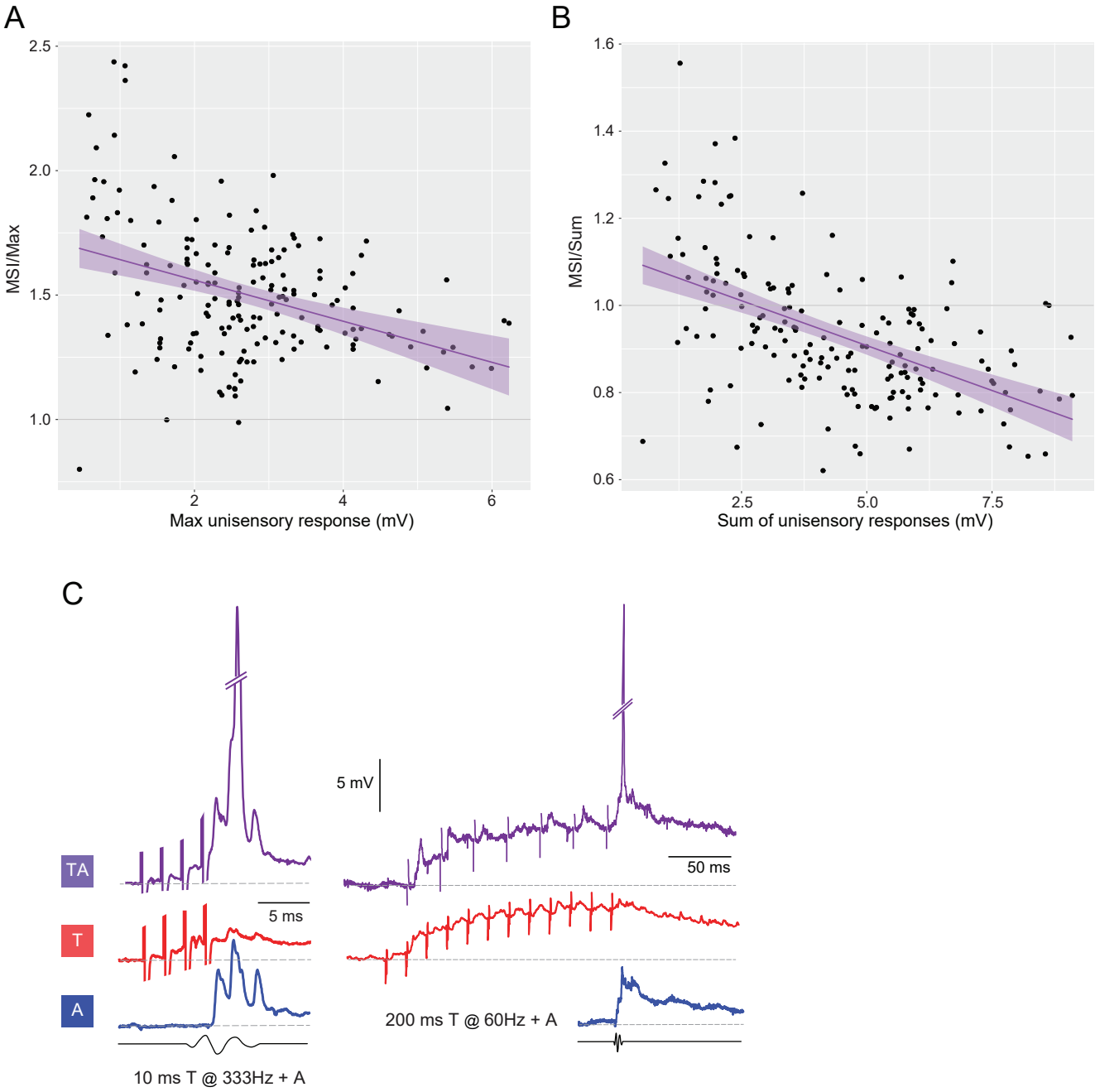
A
MSI/Max
2.5
2.0
1.5
1.0
2
4
6
Max unisensory response (mV)
B
MSI/Sum
1.6
1.4
1.2
1.0
0.8
0.6
2.5
5.0
7.5
Sum of unisensory responses (mV)
C
TA
T
A
5 ms
10 ms T @ 333Hz + A
5 mV
50 ms
200 ms T @ 60Hz + A
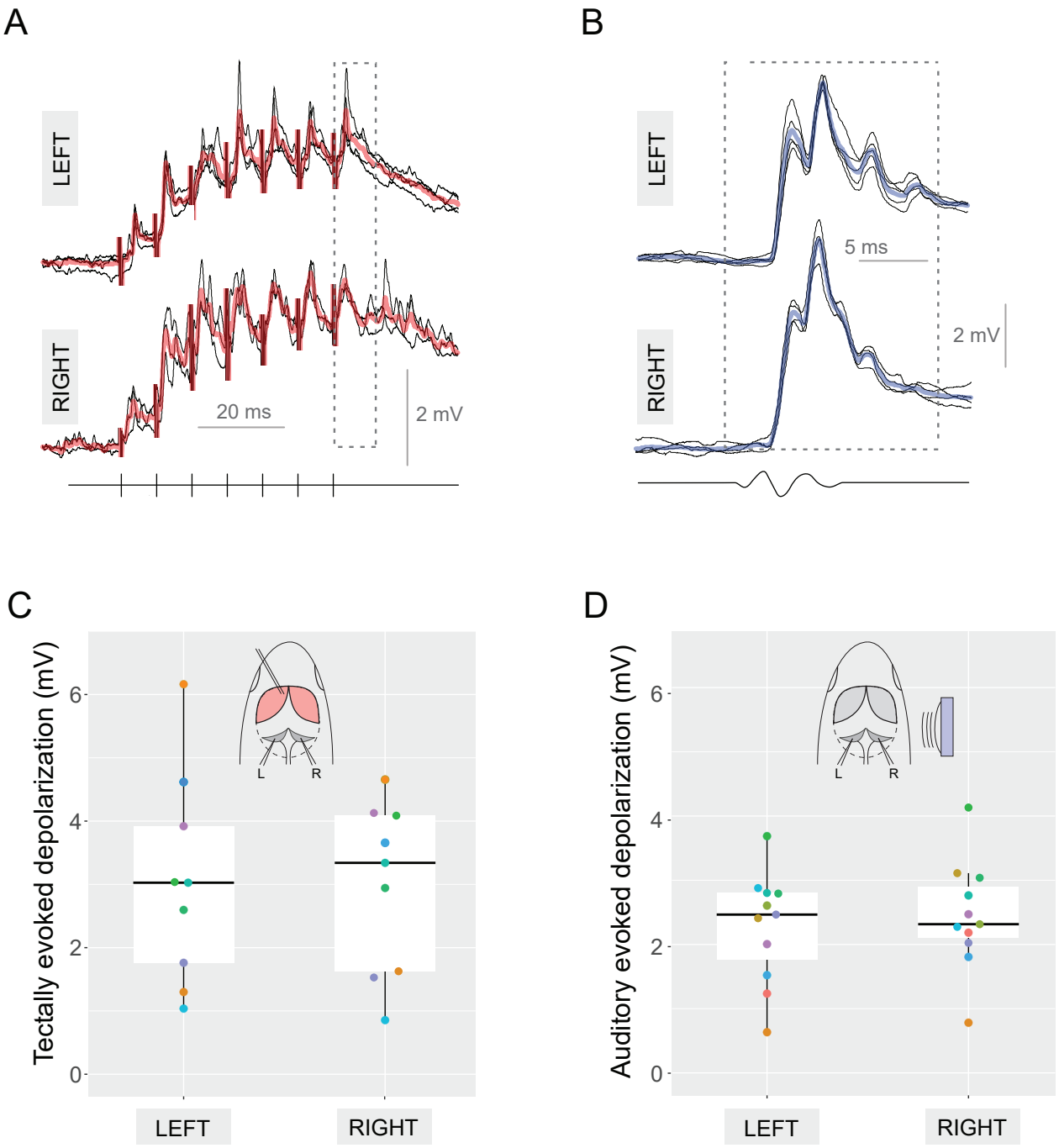
Supplementary Figure 1